Defects in self-organized criticality: A directed coupled map lattice model

Bosiljka Tadić [1,*] and Ramakrishna Ramaswamy [2,†]
[1] *Jožef Stefan Institute, P.O. Box 3000, 1001-Ljubljana, Slovenia*
[2] *School of Physical Sciences, Jawaharlal Nehru University, New Delhi 110 067, India*
(Received 13 November 1995; revised manuscript received 2 April 1996)

We study a directed coupled map lattice model in $d=2$ dimensions, with two degrees of freedom associated with each lattice site. The two freedoms are coupled at a fraction c of lattice bonds acting as quenched random defects. The system is driven (by adding ''energy,'' say) in one of the degrees of freedom at the top of the lattice, and the relaxation rules depend on the local difference between the two variables at a lattice site. In the case of conservative dynamics, at any concentration of defects the system reaches a self-organized critical state with universal critical exponents close to the mean-field values $\tau_t=1$, $\tau_s=2/3$, and $\tau_n=1/2$, for the integrated distributions of avalanche durations (t), size (s), and released energy (n), respectively. The probability distributions follow the general scaling form $P(X,L)=L^{-\alpha}\mathcal{P}(XL^{-D_X})$, where $\alpha\approx 1$ is the scaling exponent for the distribution of avalanche lengths, X stands for t, s, or n, and D_X is the (independently determined) fractal dimension with respect to X. The distribution of current through the system is, however, nonuniversal, and does not show any apparent scaling form. In the case of nonconservative dynamics—obtained by incomplete energy transfer at the defect bonds—the system is driven out of the critical state. In the scaling region close to $c=0$ the probability distributions exhibit the general scaling form $P(X,c,L)=X^{-\tau_X}\mathcal{P}[X/\xi_X(c),XL^{-D_X}]$, where $\tau_X=\alpha/D_X$ and the corresponding coherence length $\xi_X(c)$ depends on the concentration of defect bonds c as $\xi_X(c)\sim c^{-D_X}$. [S1063-651X(96)01609-1]

PACS number(s): 05.40.+j, 64.60.Ht, 68.35.Rh

I. INTRODUCTION

Critical behavior in the vicinity of a second-order phase transition is known to be sensitive to the presence of quenched random defects [1]. Quenched disorder can cause a change of the universality class of the critical behavior, in the case of weak disorder, or lead to a variety of new phenomena, as in random-field systems [2]. The case of strong disorder, represented for example, by the presence of random bonds in a spin system, can lead to a multiplicity of metastable states and frustration, as in spin glasses [3].

In contrast to conventional critical phenomena in systems that are tuned to a critical point by varying one or more external parameters, much recent work [4] has examined the behavior of extended open dynamical systems (sandpile cellular automata being a good example) that tend to self-organize into metastable states with long-range spatial and temporal correlations. Such *self-organized criticality* (SOC) in a system that is not tuned to a critical point can be expected to be somewhat more robust and less sensitive to perturbations.

The question of relevance of such perturbations in SOC is of considerable interest. A dynamic renormalization group study of spatially continuous models [5], which are believed to describe some aspects of self-organization found in cellular automata, shows that loss of translational invariance due to quenched disorder is a relevant perturbation for SOC. Similar considerations apply to the role of conservation laws in the evolution rules of such systems. Various examples studied so far [6] reveal, however, that having a conservation law in the dynamics is neither a sufficient nor a necessary condition for the critical state to appear.

We explore some aspects of these questions in the present work, where we introduce and study a *two-degree-of-freedom* (or *two-color*) directed coupled map lattice model on a two-dimensional square lattice. In our system there are two variables associated with each lattice site, and these two freedoms are practically independent in the evolution, except at a random fraction c of the lattice bonds, which act as quenched random defects. This model (termed model B in earlier work [7]) provides a simple example of a situation wherein quenched disorder acts differently from annealed disorder [8]. Similar models have also been studied in the context of signal transmission in a neural network [9].

The system is driven—by adding ''energy,'' say—to one of the degrees of freedom at a random site at the top of the lattice. Instabilities can be caused when the difference between the two variables at a site exceeds a threshold value, in which case a relaxation occurs, and the total energy accumulated in both states at an unstable site is transferred to the forward neighboring sites, creating an avalanche. Partitioning of the energy between the states at neighboring sites depends on the kind of bond (defect or normal) connecting these sites with the unstable neighbor (see Sec. II for details of the dynamics). Avalanches can be characterized through the usual indicators such as duration t, defined as the number of steps the instability progresses toward the lower boundary of the lattice, and size s, the number of lattice sites affected. In addition, we also monitor the total energy released in an avalanche (or the number of relaxations) n, as well as the total number of particles leaving the system at the lower boundary, i.e., the outflow current J.

Both conservative and nonconservative situations are possible by altering the energy transfer at defect bonds. The

*Electronic address: bosiljka.tadic@ijs.si
†Electronic address: rama@jnuniv.ernet.in

present numerical simulations, combined with a scaling analysis of the results, help in determining the conditions under which the coupled map lattice (CML) reaches a SOC state, and also the universality class to which the critical state belongs. When the dynamics is conservative, i.e., the total energy that is removed from one site appears at its neighbors, the system self-organizes into a critical state with universal scaling exponents. On the contrary, if the energy transfer is incomplete at defect bonds, our results suggest that the system is subcritical, with a finite coherence length that depends on the defect concentration c. We determine a scaling function for the distribution of size and duration of avalanches.

The case of site defects in a critical-height sandpile automaton has been examined in previous work [7,10], where we showed that the presence of nonconserving defects can lead to a loss of SOC. Site defects (either annealed or quenched) introduce a coherence length in the problem, which diverges as the concentration of defects vanishes; the relevant exponents can be derived exactly [11], since the directed Abelian sandpile with defects can be viewed as a random branching process.

In Sec. II we introduce the model and define the scaling forms of various distributions. Results are given in Sec. III for conservative dynamics and in Sec. IV for the case of nonconservative dynamics, followed by a short summary and discussion of the results in Sec. V.

II. DYNAMICAL MODEL AND SCALING

The coupled-map lattice studied here is patterned on the two-dimensional directed Abelian sandpile cellular automaton [12], which is a simple example of an exactly solvable system exhibiting SOC. We associate two dynamical variables (h_1,h_2), which for convenience can be termed energies, with each lattice site of a two-dimensional directed square lattice of linear size L. The relaxation process at lattice site (i,j) is determined by the actual values of (h_1,h_2), as follows. If the absolute value of the *difference* between h_1 and h_2 exceeds a critical value d_c, i.e.,

$$|h_1(i,j)-h_2(i,j)|\geq d_c, \tag{1}$$

then the site (i,j) becomes unstable and both h_1 and h_2 are reset to zero,

$$h_1(i,j)\to 0, \quad h_2(i,j)\to 0. \tag{2}$$

We take $d_c=2$ in our simulations. The lattice sites are connected by bonds that can be either positive or negative, and these affect the subsequent relaxation rules differently. (We consider the situation when most bonds are positive, and a fraction c of negative bonds are distributed at random and act as defects.) Along positive bonds,

$$h_1(i+1,j_\pm)\to h_1(i+1,j_\pm)+[h_1(i,j)+h_2(i,j)]/2, \tag{3}$$

and along negative bonds,

$$h_2(i+1,j_\pm)\to h_2(i+1,j_\pm)+[\lambda h_1(i,j)+h_2(i,j)]/2. \tag{4}$$

$j_\pm=j\pm[1-(-1)^i]/2$ and $(i+1,j_\pm)$ label the two downstream neighbors of (i,j). As can be seen, for $\lambda=1$ the total energy h_1+h_2 disappearing from site (i,j) reappears in either h_1 or h_2 of the forward neighbors regardless of the parity of the connecting bonds—the dynamics is conservative. If $\lambda<1$, some amount of energy is lost along the negative bonds and the dynamics is nonconservative. This case is considered in Sec. IV below.

The system is driven by adding an energy unit at random sites at the input at the top (i.e., along the row $i=1$),

$$h_1(1,j)\to h_1(1,j)+1, \tag{5}$$

and allowed to proceed following the rules embodied in Eqs. (1)–(4) until there are no further instabilities. This constitutes an avalanche. Starting from an initially random configuration, the system eventually reaches a SOC state [7–9] when there are avalanches of all duration and size scales. These can be characterized through the following four quantities.

(a) The length ℓ is the total distance that an avalanche propagates. $P(\ell)\sim\ell^{-(1+\alpha)}$ is the probability distribution of avalanches of length ℓ.

(b) The size s is the number of sites at which relaxation occurs in one avalanche. $D(s)\sim s^{-\tau_s}$ is the distribution of avalanches of size s or greater.

(c) In sandpile automata a distinction can be made between the number of particles toppled and the number of sites involved in an avalanche [13]. The number of particles that topple at one unstable site in our model is $n(i,j)=h_1(i,j)+h_2(i,j)$ in the conservative case [cf. Eqs. (1)–(4)], and this quantity varies from site to site. Therefore the total number of relaxations, n, defined as $n=\Sigma_{(ij)}n(i,j)$, is not simply proportional to the size s, which is defined as $s=\Sigma_{(ij)}1$, where the sum in both cases runs over all sites involved in an avalanche. This introduces the distribution of avalanches $Q(n)\sim n^{-\tau_n}$ of the number of relaxations $\geq n$.

(d) The duration of an avalanche, t, is described by the distribution $P(t)\sim t^{-(1+\tau_t)}$. From finite-size scaling arguments [14] in the SOC state these distributions should obey the following general scaling form:

$$P(X,L)=L^{-\alpha}\mathcal{P}(XL^{-D_X}), \tag{6}$$

where α is the above-defined exponent of the distribution of lengths $P(\ell)$, and X represents s, n, or t. Correspondingly, D_X stands for the appropriate fractal dimension, which is defined via the following relations:

$$\langle s\rangle_\ell\sim\ell^{D_s}, \tag{7}$$

$$\langle n\rangle_\ell\sim\ell^{D_n}, \tag{8}$$

and

$$\langle t\rangle_\ell\sim\ell^{D_t}, \tag{9}$$

where $\langle\rangle_\ell$ denotes an average over all avalanches of selected length ℓ (i.e., avalanches that exactly terminate on the ℓth row).

Note that D_t is the dynamic exponent (usually denoted z). In the present directed model, since avalanches propagate only in the forward direction, the duration is equivalent to the length. The dynamic exponent is thus exactly 1, and

$\tau_t \equiv \alpha$. This need not be the case when the relaxation rules are more complex [7]. Furthermore, all the exponents are not independent, since the scaling relations [7]

$$\alpha = D_s \tau_s = D_n \tau_n = \tau_t D_t \tag{10}$$

are valid for the exponents of integrated distributions as defined above.

In the present work we consider quenched disorder; i.e., our numerical results are averaged over several sample lattices, each prepared by distributing defect bonds with concentration c. We keep the lattice configuration fixed for a large number of Monte Carlo steps (which is equal to number of events), and consider both cases of conservative and nonconservative transfer at defect bonds. In order to minimize effects of boundaries, we chose so-called free boundaries in the perpendicular direction. This is achieved by using a lattice of size $2L \times L$ and initializing avalanches between the sites $L/2+1$ and $3L/2$ at top. According to the above dynamic rules, only escape of energy is possible at the bottom of the lattice between sites 1 and $2L$. Results of our numerical studies are presented in Secs. III and IV.

III. CONSERVATIVE DYNAMICS

For $\lambda = 1$ in Eq. (4), the dynamics is conservative. The system reaches the SOC state, which we characterize through the quantities enumerated in Sec. II. It is sufficient to consider the disorder regime of $c \leqslant 0.5$ owing to the symmetry $c \to 1-c, h_1 \to h_2$. When $c = 0$ this model reduces to a directed Abelian sandpile automaton in the h_1 degree of freedom, and the empty state in the other degree of freedom, $h_2 = 0$ at all sites. For nonzero c, the SOC state is more difficult to describe. We study the histogram of total energy per site, defined as $E = h_1 + h_2$ after a relaxation event, for both $c = 0$ and a few values of $c \neq 0$. In the case $c = 0$ it takes nonzero values at the interval $[0,1]$, however, for $c \neq 0$ much larger values of energies occur, although with smaller probability compared to those between $E = 0$ and $E = 1$. Spreading of the distribution in the presence of defect bonds $c \neq 0$ indicates that the critical state is realized via multiplicity of configurations of the dynamic variables h_1 and h_2, which depends on c.

We observe, however, that the concentration of defect bonds $c \neq 0$ does *not* appear to affect the critical exponents characterizing the SOC state in this model. The distribution of lengths of the relaxation clusters $P(\ell)$, size $D(s)$, and

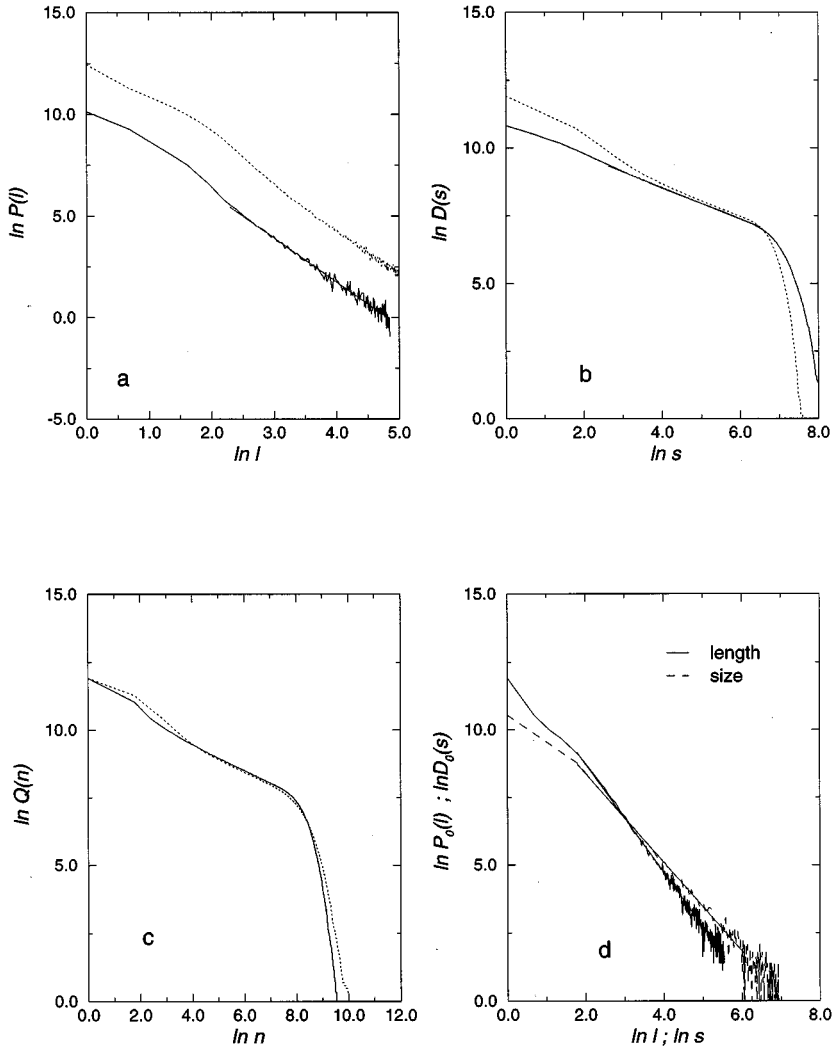

FIG. 1. Double logarithmic plot of (a) distribution of avalanche lengths $P(\ell)$ vs ℓ; (b) integrated distribution of avalanche sizes $D(s)$ vs s; (c) integrated distribution of number of relaxations $Q(n)$ vs n, for two concentration of defect bonds $c = 0.1$ (dotted curves) and $c = 0.5$ (solid curves); (d) distributions of avalanche lengths and sizes (not integrated), $P_0(\ell)$ vs ℓ and $D_0(s)$ vs s, respectively, for the case $c = 0$.

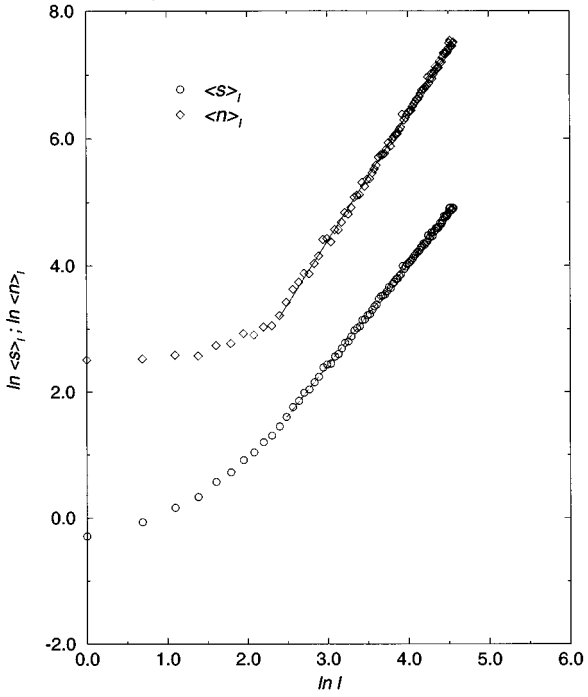

FIG. 2. Double-logarithmic plot of the average values of size $\langle s\rangle_\ell$ and number of relaxations $\langle n\rangle_\ell$ in clusters of selected length ℓ, vs ℓ.

number of relaxations $Q(n)$ for two different concentrations of defect bonds $c=0.1$ and $c=0.5$ are shown in Fig. 1. The exponents are numerically determined (with the statistical error bars) to be $\alpha=1.051\pm0.044$, $\tau_s=0.650\pm0.028$, and $\tau_n=0.509\pm0.004$, *independent* of defect concentration c, suggesting that this model has universal criticality.

In Fig. 1(d) the distributions for length and size of avalanches $P_0(\ell)$ and $D_0(s)$ are shown for the case $c=0$. Slopes of these curves, corresponding to the above defined exponents $1+\alpha$ and $1+\tau_s$, respectively, are estimated as 1.998 ± 0.019 and 1.58 ± 0.04. For τ_n we find the value 0.528 ± 0.022.

In Fig. 2 we present results for the time averaged size $\langle s\rangle$ and relaxed energies $\langle n\rangle$ in avalanches of a fixed (selected) length ℓ. According to Eqs. (7) and (8), slopes of these curves determine the mass-to-scale ratios (fractal dimensions) D_s and D_n, which are determined to be $D_s=1.615\pm0.007$ and $D_n=1.997\pm0.008$. Plotted are the results for $c=0.5$, but it was checked that the values of the exponents remain concentration independent.

In order to fully characterize the self-organized critical state, we have determined the various exponents and the corresponding scaling functions. The results of the finite-size scaling fit according to Eq. (6) are shown in Figs. 3 and 4, where we used $\alpha=1.04$, $D_s=1.62$, and $D_n=2$.

In contrast to many sandpile models, where the number of topplings (corresponding to n in our model) is expected to scale with a fractal exponent [15], we find that the relaxation rules (1)–(4) lead to a rather classical exponent $D_n=2$. The distributions of the size of relaxation clusters $D(s,L)$ and the distribution of the number of relaxations $Q(n,L)$ satisfy the finite-size scaling form (6) with the above determined exponents.

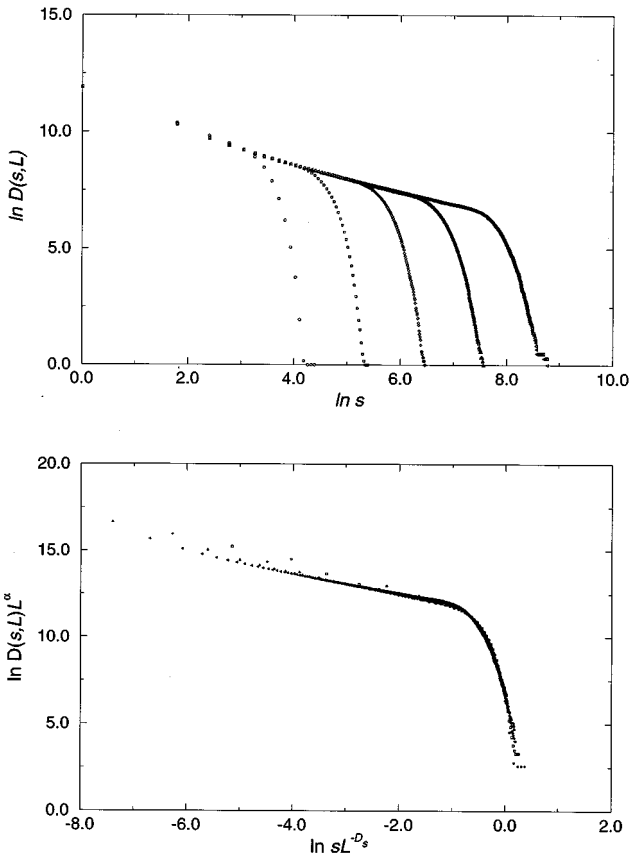

FIG. 3. Double-logarithmic plot of the integrated distribution of size of avalanches $D(s,L)$ vs size s for several different values of lattice size L (above), and the corresponding finite-size scaling plot according to Eq. (6) (below).

The distribution of outflow current $G(J,L)$, which is the current that flows over the lower boundary of the system, rather than having a power-law dependence on J, fulfills the finite-size scaling form [14]

$$G(J,L)=L^{-\beta}\mathcal{G}(JL^{-\phi}), \tag{11}$$

where $\beta=2\phi$ in the stationary state. In Fig. 5 we show the distribution $G(J,c,L)$ for (a) fixed concentration of defect bonds $c=0.5$ and various lattice sizes, and (b) for fixed lattice size $L=192$ and various concentrations of defects c. The distribution $G(J,c,L)$ for finite concentration c of defect bonds is rather localized, as opposed to the case $c=0$, where the distribution is broad. We find no apparent finite-size scaling for $G(J,c,L)$ for nonzero values of c.

We end this section with a comment on numerical values of the critical exponents. Our results suggest that the values of the exponents for avalanche duration and for the number of relaxations are close to those in the mean-field SOC [16,17]—in our notation, $1+\tau_t\approx2$, and $1+\tau_n\approx3/2$ [18]. The mean-field universality class [16] is obtained in self-organizing sandpile models where (i) there is a frontlike spreading of avalanches with noninteracting sites at the front, and (ii) a global constraint exists, which maps the dynamic model to a *critical* branching process. Although our model has somewhat more complex evolution rules, the exponents

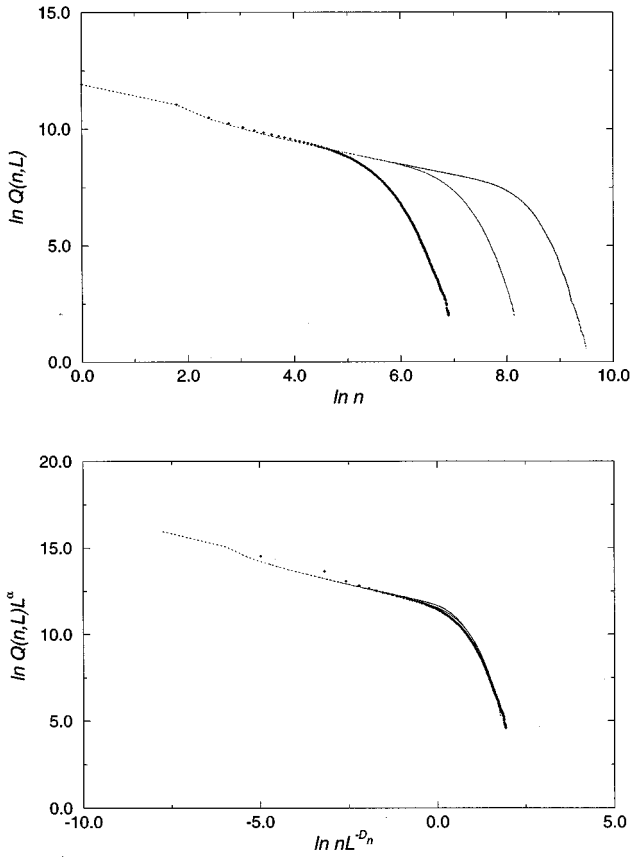

FIG. 4. Same as Fig. 3 but for the integrated distribution of number of relaxations $Q(n,L)$ vs n for three different values of lattice size L (top), and the corresponding finite-size-scaling plot according to Eq. (6) (bottom).

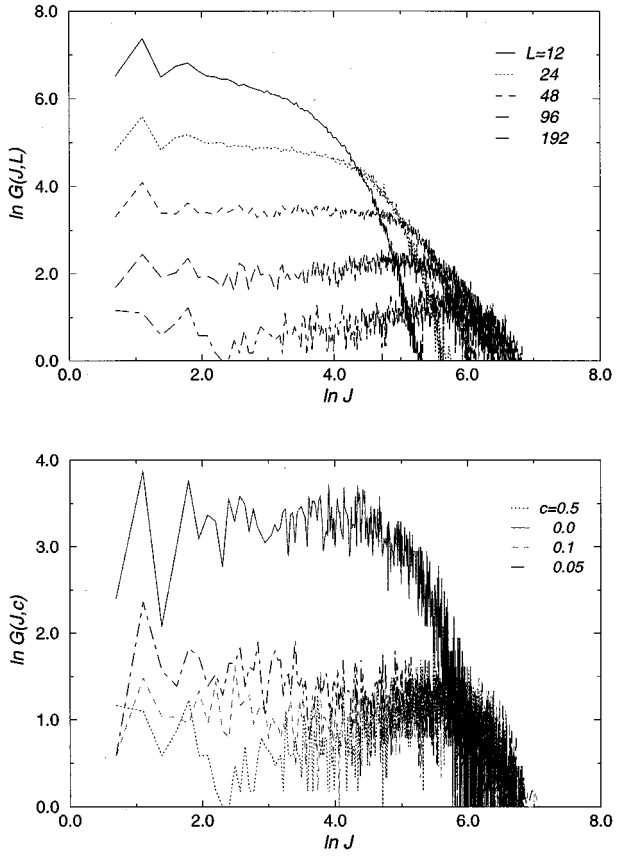

FIG. 5. Double-logarithmic plot of the distribution of outflow current $G(J,c,L)$ vs current J for fixed concentration of defect bonds $c=0.5$ and various lattice sizes L (top), and for fixed $L=192$ and various concentrations c as indicated (bottom).

appear to be in the same universality class. (Note that in our model, compared to the sandpile automata, there is one more independent exponent, i.e., $1+\tau_s \approx 5/3$.)

IV. THE CASE OF NONCONSERVATIVE DEFECTS

When $\lambda \neq 1$ in Eq. (4) the model becomes nonconservative at defects bonds. By studying the probability distributions of duration $P(t,c,L)$ and size $D(s,c,L)$ of avalanches for various concentrations of nonconserving defect bonds c, we find that SOC behavior is lost as soon as energy conservation is lost.

One quantity that proves to be useful in characterizing the present situation is the average number of relaxations $\langle n(\ell) \rangle$, which occur in all kinds of clusters up to length ℓ (which is different from the average number of relaxations in clusters of selected length, which was considered above). In the case of conservative dynamics this quantity exhibits a power law [7]

$$\langle n(\ell) \rangle \sim \ell^{D_n(1-\tau_n)}, \tag{12}$$

independent of the degree of disorder.

Numerical results are obtained by fixing $\lambda = 0.9$ and varying c. Shown in Fig. 6 are results for the average number of topplings $\langle n(\ell) \rangle$, for the conservative case (open circles) as well as for $\lambda < 1$ and different values of c, where it can be seen that the power law is lost and the results depend on the concentration of defect bonds c (the remaining lines in Fig. 6).

We further study the effects of concentration of defect bonds on the distributions of size and duration (or length) of the relaxation clusters. In Figs. 7(a) and 7(b) these distributions are shown for $L=128$ and for few values of c. The following general scaling form is appropriate for the case of lattice disorder [10]:

$$P(X,c,L) = \ell^{\lambda_P} P(\ell^{\lambda_X} X, \ell^{\lambda_c} c, \ell^{-1} L), \tag{13}$$

where λ_i, $i \equiv X,c,P$, are the scaling exponents for the variables X, concentration of defect bonds c, and the generalized scaling function itself P, respectively. By chosing $\ell^{-1} L \sim 1$ we have

$$P(X,c,L) = L^{\lambda_P} P(L^{\lambda_X} X, L^{\lambda_c} c, 1), \tag{14}$$

which is appropriate for the finite-size scaling analysis. The scaling function on the right-hand side of Eq. (14) is numerically determined from the data for various values of L and c. As the analysis in Sec. III shows, in the case of conservative defects this scaling function is independent on c and depends on L as

$$P(X,c,L) = L^{\lambda_P} \mathcal{P}(L^{\lambda_X} X). \tag{15}$$

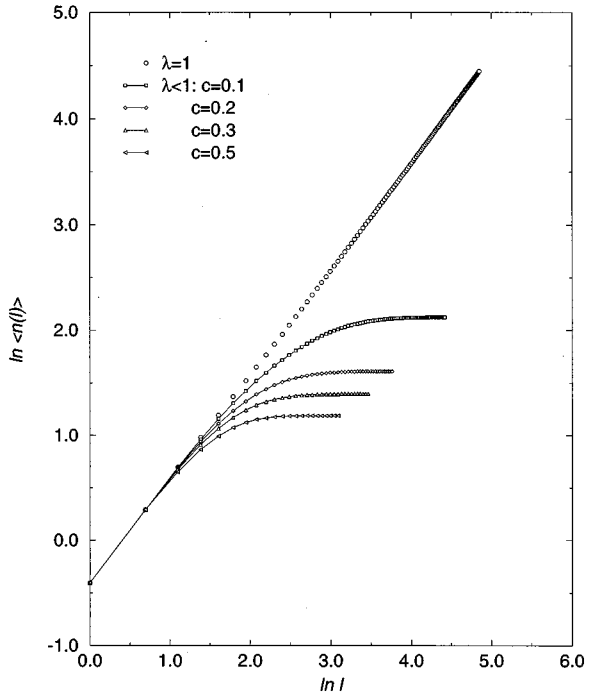

FIG. 6. Double-logarithmic plot of the average number of relaxations up to distance ℓ from the top of pile $\langle n(\ell)\rangle$ vs ℓ for conservative defects $\lambda=1$ (open circles) and for $\lambda<1$ and various concentrations of nonconservative defects c as indicated.

[This is exactly Eq. (6), where the scaling exponents are identified as $\lambda_P=-\alpha$ and $\lambda_X=-D_X$.] This implies that the scaling exponent of the conservative defects in the expression (14) is $\lambda_c<0$, and thus, these types of defects are irrelevant for SOC. [This conclusion is also supported by the fact that numerical values of the exponents used in the scaling fits in Sec. III satisfy the theoretical scaling relations (10).] On the contrary, when the defects violate the conservation law of the dynamic rules, the results are quite different. The distributions [cf. Figs. 7(a) and 7(b)] depend explicitly on c, and the finite-size scaling fit (15) is inappropriate. (Even fitting to this functional form gives poor results, the badness of the fit depending on c.) In order to study these effects in a more quantitative way, we fix L and chose another variable in the general scaling form (13), namely, $\ell^{\lambda_X}X=1$, leading to

$$P(X,c,L)=X^{-\lambda_P/\lambda_X}P(1,X^{-\lambda_c/\lambda_X}c,X^{1/\lambda_X}L), \qquad (16)$$

which could be also written as

$$P(X,c,L)=X^{-\tau_X}\mathcal{P}[X/\xi_X(c),X/L^{D_X}]. \qquad (17)$$

with identification $\lambda_X=-D_X$, $\tau_X=\lambda_P/\lambda_X(=\alpha/D_X)$, and $\xi_X(c)=c^{\lambda_X/\lambda_c}=c^{-D_X/\lambda_c}$. Here $\xi_X(c)$ is the corresponding coherence length, which, as is evident in Fig. 6, varies with the concentration of defect bonds c. By fitting the numerical data in Figs. 7(a) and 7(b) to the scaling form (17) we determine the c dependence of $\xi_X(c)$, which appears to be most satisfactorily described as $\xi_\ell=1/c$ and $\xi_s=c^{-D_s}$, for the distributions of length and size, respectively, $\tau_\ell\equiv\alpha$, τ_s, and D_s being the exponent determined in Sec. III. The results are shown in Figs. 7(c) and 7(d). With this result in hand, we may conclude that the numerical value of the scaling exponent λ_c in the expression $\xi_X(c)=c^{-D_X/\lambda_c}$ is $\lambda_c=1$, within numerical error. That is, defects that violate the conservation law of the dynamics are *relevant* perturbations for the SOC state. Owing to the factor X/L^{D_X} in the scaling function (17), we restrict the fits to rather large concentrations c [see Figs. 7(a) and 7(b)] in order to satisfy the relation $\xi/L\ll 1$. It is interesting to note that the scaling region where Eq. (17) applies is restricted to a finite range of values of $c<c^*$ in the vicinity of the point $c=0$. For instance, the curves corresponding to $c=0.5$ in Figs. 7(a) and 7(b) do not obey the scaling form (17), indicating that $c^*<0.5$. In the limit $c=0$ the dynamics becomes conservative and true SOC reappears [cf. Fig. 1(d)].

Similar scaling fits were introduced earlier in Ref. [10] in a simple critical height model with site defects. Here we demonstrate that in the case of more complicated relaxation rules with nonconservative bond defects, the coherence lengths have the same general dependence on the concentration of defects, namely, $\xi_X(c)\sim c^{-D_X}$, where, in principle, the values of the exponents D_X depend on the dynamic model. Exact expressions for the coherence lengths in the case of the directed Abelian sandpile model with site defects have been obtained by mapping the model to a random branching process [11].

V. SUMMARY AND DISCUSSION

In this work we have further explored the role of defects in models of self-organized criticality. In the case of sandpiles with random site defects [10], the dynamics is altered locally at defect sites. The situation of defects having a more global influence is also of interest, and we achieve this in the present two-color random bond model. Our coupled map lattice has two degrees of freedom associated with each lattice site. Disorder is present in the form of quenched random bond defects, which can be both conserving ($\lambda=1$) or nonconserving ($\lambda\neq 1$). There is a preferred direction of transport, which serves to simplify the dynamical evolution rules, leading to a minimal model with quenched random bonds. The evolution rules of the model are motivated by the signal transmission in a *directed* neural network, where quenched disorder is known to play an important role. Preliminary studies [7,8] have indicated that annealed and quenched random disorder can behave differently, and our model is one of the simplest examples. Similar self-organizing coupled-map lattice models have been studied to some extent in the literature as models of more realistic sandpiles [19], abstract examples of adaptive self-organizing systems [20], vector-state models [21], and as nondirected neural networks [9].

With conservation, $\lambda=1$, in the limit of no disorder, $c=0$, the model becomes an Abelian CML with single dynamic variable (energy $h\equiv h_1$), and reaches a SOC state in which the distribution $D(h_1)$ is nonzero at the interval [0,1], and $h_2=0$ everywhere. For nonzero concentration of defect bonds ($c\neq 0$), an additional state h_2 is generated at a fraction c of lattice sites, which affects the propagation of avalanches. The SOC state is again reached under the condition that the total energy (consisting of h_1+h_2) accumulated at an unstable site is completely transferred to its neighbors. Conservation of h_1 by itself appears to be insufficient. The

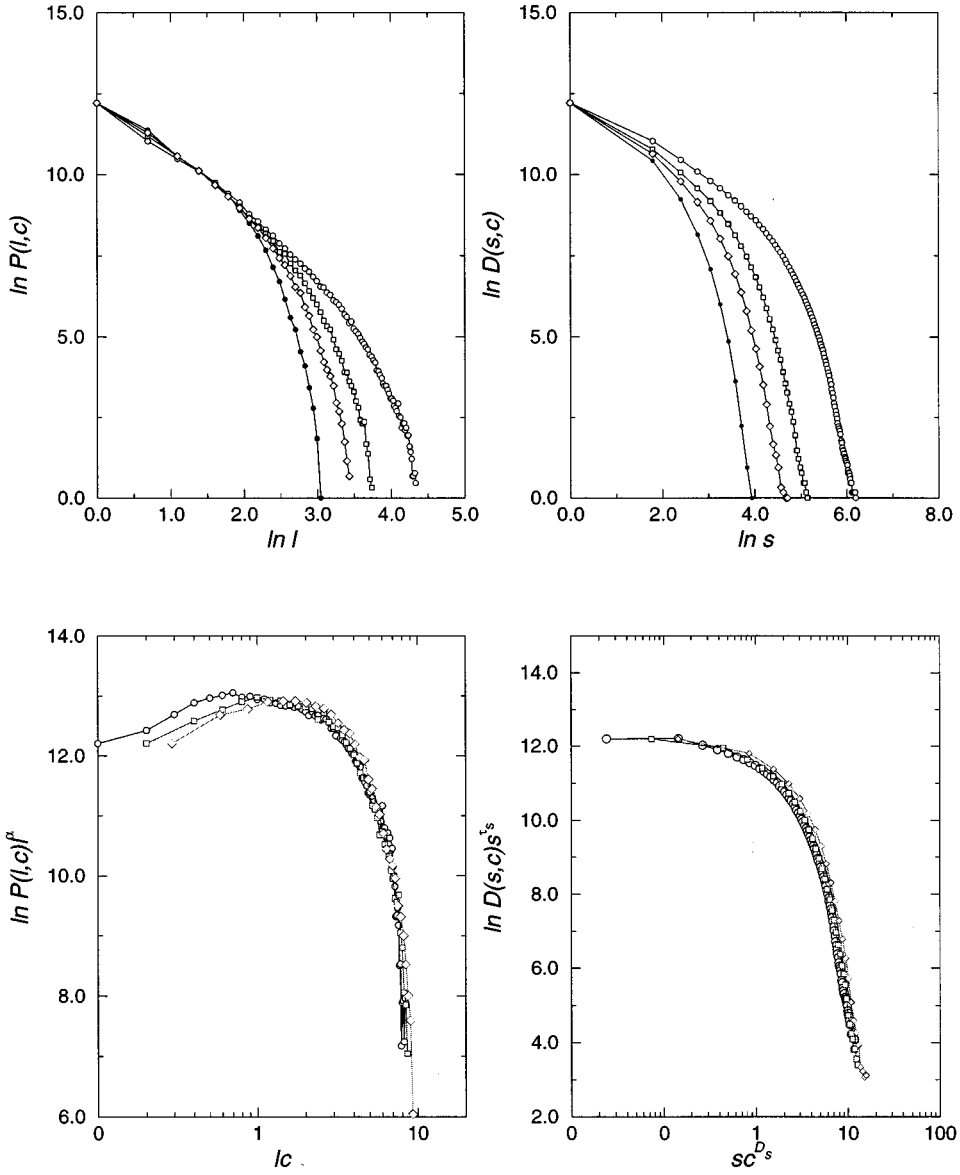

FIG. 7. Top: Double-logarithmic plot of the distribution of length $P(\ell,c)$ vs length ℓ and the integrated distribution of size $D(s,c)$ vs size s of avalanches for few concentrations of nonconservative defects (from right to left: $c=$ 0.1, 0.2, 0.3, and 0.5) and fixed $L=$ 128. Bottom: Scaling plots of the same distributions for $c=0.1$, 0.2, and 0.3 according to Eq. (17).

critical state has a more complex structure, evidenced by a spread in the distribution of the values of h_1 and h_2, the width of the distribution being a strong function of c, as is shown in Fig. 8. However, the critical *exponents* characterizing the SOC state appear to be *independent* (within numerical uncertainty) of the concentration of defects c. By redistribution of energies, the system adjusts to the presence of defects and thus maintains its criticality. Numerical values of these exponents suggest that both $c=0$ and $c>0$ models belong to the mean-field SOC universality class [16,17]. In particular, exponents for the distributions of the duration (or length) of relaxation clusters and the number of relaxations are close to the exact values $1+\alpha\approx 2$ and $1+\tau_n\approx 3/2$, respectively. Due to the more complex dynamical rules in our CML model when $c\neq 0$, we can distinguish between τ_n and the exponent of the distribution of size of avalanches τ_s, which are equivalent in Abelian sandpile models [13]; the present results suggest that $1+\tau_s\approx 5/3$.

By modifying the relaxation rules in a way such as to permit incomplete energy transfer at defect bonds (i.e., h_2 is not conserved while h_1 remains conserved), we study the significance of the conservation on the SOC state. Similar to the case of sandpile automata with site defects, the self-organizing CML is driven out of the critical state (cf. Fig. 7), with the concentration of defect bonds c playing the role of a control parameter. It should be stressed that in our model the lack of particle conservation is linked to the quenched defect structure: with the present rules, it is not possible to have a nonconservative model that does not also have defects. This enables the quantitative analysis of the subcritical state in terms of varied coherence length $\xi_X(c)$, as done in Sec. IV. It is interesting to note that the distributions in Figs. 7(a) and 7(b) do not depend on the degree of nonconservation [which is indexed by the parameter λ in Eq. (4); see also Ref. [7]], but only on the spatial distribution of defect bonds (indexed by the parameter c). It is very possible that a cellular automaton with otherwise nonconservative dynamics (there are by now several examples in the literature whereby one can implement nonconservative evolution rules and reach a SOC state [6]) becomes subcritical upon introduction of conserva-

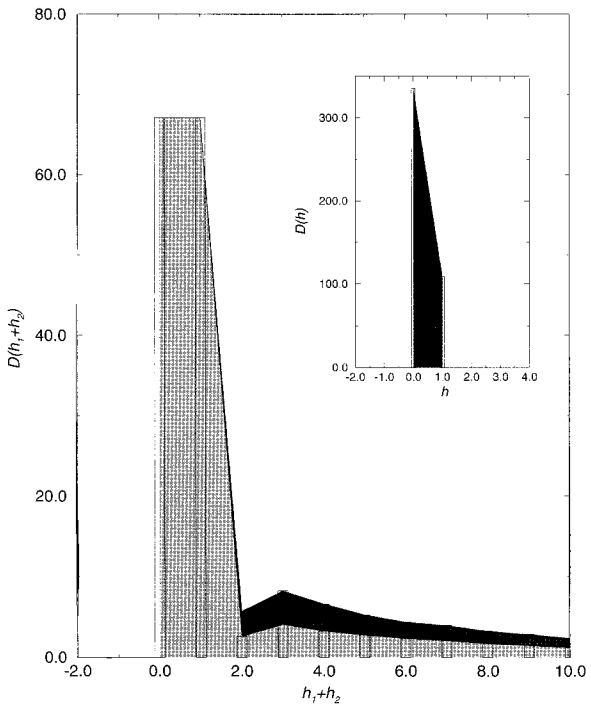

FIG. 8. Distribution of enegries per site $D(h_1+h_2)$ vs h_1+h_2 for two concentrations of defect bonds $c=0.1$ (front) and $c=0.5$ (back). Inset: Same distribution in the absence of defects $c=0.0$.

tive defects, similar to our model in Sec. IV. We have not considered this kind of model in the present work. Similarly, the question of the relevance of the spatial correlation of defects for the SOC state is left for future study. The coherence lengths are tuned by the concentration of defect bonds according to the general law $\xi_X(c)\sim c^{-D_X}$. In the case of site defects, the sandpile automaton can be mapped onto a random branching process, and the exact expression for the $\xi_t(c)$ has been derived (see Ref. [11] for details). We suggest that the scaling form (17) together with the expression $\xi_X(c)\sim c^{-D_X}$ for the coherence lengths applies for the probability distributions in a wider class of *subcritical* self-organizing systems.

In contrast to spatially continuous models in which disorder is always a relevant perturbation [5], our numerical results suggest that the present coupled-map lattice model self-organizes into a universality class of the mean-field SOC, which is robust to quenched random bonds, as long as the dynamics is conservative. The conservative defects influence the distribution of energies per site in the critical state and alter the nonuniversal quantities, such as outflow current, whereas the universal properties, i.e., critical exponents and scaling functions, are not affected. However, a question remains as to whether other types of defects, such as those studied in discrete sandpile automata in Refs. [7,22], combined with different dynamic rules, may lead to continuous tuning of the universality class with a parameter in CML models.

ACKNOWLEDGMENTS

This work was supported by the Ministry of Science and Technology of the Republic of Slovenia, and the DST, India under Grant No. SP/S2/MO5/92.

[1] R. B. Stinchcombe, in *Phase Transitions and Critical Phenomena*, Vol. 7, edited by C. Domb and J.L. Lebowitz (Academic, New York, 1983).
[2] For a recent review see W. Kleemann, Int. J. Mod. Phys. B **7**, 2469 (1993).
[3] K.H. Fisher and J.A. Hertz, *Spin Glasses* (Cambridge University Press, Cambridge, 1991).
[4] P. Bak, C. Tang, and K. Wiesenfeld, Phys. Rev. Lett. **59**, 381 (1987); Phys. Rev. A **38**, 364 (1988).
[5] J. Toner, Phys. Rev. Lett. **66**, 679 (1991).
[6] See, e.g., S.S. Manna, L. Kiss, and J. Kertész, J. Stat. Phys. **61**, 923 (1990); K. Christiansen and Z. Olami, Phys. Rev. A **46**, 1829 (1992); A. Corral, C.J. Pérez, A. Díaz-Guilera, and A. Arenas, Phys. Rev. Lett. **74**, 118 (1995); S.S. Manna (unpublished).
[7] B. Tadić and R. Ramaswamy, Physica A **224**, 188 (1996).
[8] B. Tadić, J. Noncryst. Solids **172-174**, 501 (1993).
[9] E.N. Miranda and H.J. Herrmann, Physica A **175**, 339 (1991).
[10] B. Tadić, U. Nowak, K.D. Usadel, R. Ramaswamy, and S. Padlewski, Phys. Rev. A **45**, 8536 (1992).
[11] J. Theiler, Phys. Rev. E **47**, 733 (1993).
[12] D. Dhar and R. Ramaswamy, Phys. Rev. Lett. **63**, 1659 (1989).
[13] S.S. Manna, J. Stat. Phys. **59**, 509 (1990).
[14] L.P. Kadanoff, S.R. Nagel, L. Wu, and S.M. Zhou, Phys. Rev. A **39**, 6524 (1989).
[15] I.M. Jánosi and A. Csirók, Fractals **2**, 153 (1994).
[16] S. Zapperi, K.B. Lauritsen, and H.E. Stanley, Phys. Rev. Lett. **75**, 4071 (1995).
[17] C. Tang and P. Bak, J. Stat. Phys. **51**, 797 (1988); D. Dhar and S.N. Majumdar, J. Phys. A **23**, 4333 (1990); S.A. Janowsky and C.A. Laberge, *ibid.* **26**, L973 (1993); H. Flyvbjerg, K. Sneppen, and P. Bak, Phys. Rev. Lett. **71**, 4087 (1993); J. de Boer, B. Derrida, H. Flyvbjerg, and T. Wettig, *ibid.* **73**, 906 (1994).
[18] These exact values are expected in the limit of infinite duration and system size. The systematic deviations of our numerical values for the exponents from the limiting laws are due to finite durations and sizes in the numerical simulations.
[19] A. Mehta, G.C. Barker, J.M. Luck, and R.J. Needs, Physica A, **224**, 48 (1996); A. Mehta and G.C. Barker, Europhys. Lett. **27**, 501 (1994).
[20] S. Sinha and D. Biswas, Phys. Rev. Lett. **71**, 2010 (1993); S. Sinha, Phys. Rev. E **49**, 4832 (1994).
[21] G. Peng, Physica A **201**, 573 (1993).
[22] S. Lübeck, B. Tadić, and K.D. Usadel, Phys. Rev. E **53**, 2182 (1996).